Special Collection

Insights Into the Mechanism of Energy Transfer with Poly (Heptazine Imide)s in a Deoximation Reaction

Alexey Galushchinskiy,[a] Katharina ten Brummelhuis,[a] Markus Antonietti,*[a] and Aleksandr Savateev*[a]

Following our previous studies on potassium poly(heptazine imide) (K-PHI), that is, catalyzed photooxidative [3+2] aldoxime-to-nitrile addition to form 1,2,4-oxadiazoles, we discovered that electron-rich oximes yield the parent aldehydes instead of target products. In this work, the mechanism of this singlet oxygen-mediated deoximation process was established using a series of control reactions and spectroscopic measurements such as steady-state and time-resolved fluorescence quenching experiments. Additionally, the singlet-triplet energy gap value was obtained for K-PHI in suspension, and the reaction scope was broadened to include ketoximes.

1. Introduction

In the last years, photoredox catalysis has become a powerful tool for synthetic chemists due to its versatility[1] and broad variety of supported single-electron transfer reactions, which range from late-stage introduction of the isotope labels[2,3] to complex transformations of organic compounds.[4,5,6] This approach allows employing radical pathways in the reaction without using toxic organometallic reagents or unstable hazardous initiators. Instead, it relies on electron transfer between substrates and a photocatalyst using abundant sacrificial electron acceptors, such as O_2 from air, and electron donors, such as ethanol derived from biomass.[7]

One of the most notable classes of currently available heterogenous photocatalysts are carbon nitrides. Being semiconductors rather than photoactive small molecules, they are mostly associated with photoelectrochemical water splitting and artificial photosynthesis,[8,9] however, recent trend shows increasing number of publications with the tag 'organic photocatalysis'.[10–12] Despite the current scope of reactions is not as broad as that for homogeneous catalysts, such as $Ru(bpy)_3Cl_2$ and $Ir(ppy)_3$, carbon nitrides in general show similar activity[13] as well as they enable unique transformations.[14] Moreover, these materials are advantageous, both in terms of

cost and handling, as they could be easily separated from reaction mixture and then re-used for multiple times.

The common feature of both molecular and semiconductor photocatalysts is that the reactions in which they are employed are mainly based on electron transfer. Few reactions that proceed via energy transfer are known, and they are mostly limited to cyclization reactions and singlet oxygen generation.[15] One example of carbon nitride-catalyzed energy transfer reaction is synthesis of 1,2,4-oxadiazoles developed by our group.[16] Potassium poly(heptazine imide) (K-PHI, Figure 1a) was used as a solid state $^1O_2$ sensitizer, which, in turn, converted aldoximes to corresponding nitrile oxides forcing them to undergo subsequent click-reaction with nitriles.
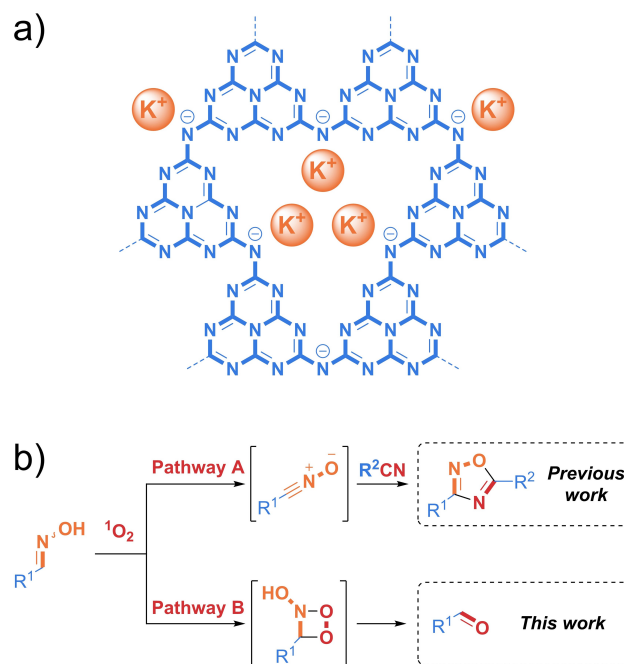
[a] A. Galushchinskiy, K. ten Brummelhuis, Prof. Dr. Dr. M. Antonietti, Dr. A. Savateev
Department of Colloid Chemistry
Max Planck Institute of Colloids and Interfaces
Am Mühlenberg 1, 14476 Potsdam (Germany)
E-mail: Oleksandr.Savatieiev@mpikg.mpg.de
Markus.Antonietti@mpikg.mpg.de

Figure 1. a) Idealized structure of potassium poly(heptazine imide) (K-PHI) layer. b) Different pathways of singlet oxygen quenching by oximes
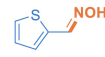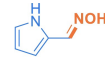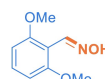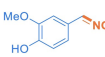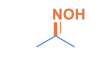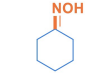
However, more electron-rich oximes failed to yield the desired [3+2]-cyclization products and instead were converted into aldehydes (Figure 1b). Herein, we investigate the mechanism of this process in greater details, as it may have synthetic value for employing oxime as a carbonyl protecting group[17] or for preparation of aldehydes and ketones from non-aromatic nitrosation products (Figure S46),[18,19] which may be valuable in case of sensitive substrates that are unstable in regular oxime hydrolysis conditions.

2. Results and Discussion

For our studies, we selected several aldoximes **1a–e** from our previous work that were resistant to oxidative dehydrogenation

(Figure S45, Table 1), as well as some common ketoximes **1f–h**, **1j–l** to investigate how the absence of aldoxime C–H proton influences the reaction pathway and structure of the final products. Oxime **1i** was chosen as a substrate for mechanistic studies due to the fact that parent coumarin **2i** can be easily distinguished from the oxi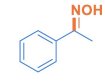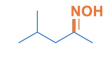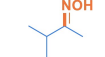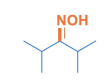me **1i** in the NMR spectrum of the crude reaction mixture. Moreover, coumarin **2i** is significantly more fluorescent compared to the oxime **1i**. Therefore, conversion of oxime **1i** into the corresponding ketone may serve as an example of switch-ON fluorescence reaction actuated by photochemistry or photocatalysis, which previously has been enabled by chemical oxidant – trichloroisocyanuric acid.[20] Finally, oxygen-18 isotopomer **1g-^{18}O** was synthesized to check our initial hypothesis if reaction proceeds via [2+2]-cycloaddition of $^1O_2$ to the oxime C=N bond.

Table 1. Scope of oximes **1a–h**.[a]

Entry	Substrate		Yield (Conversion) [%] Blue LED, 461 nm K-PHI, 24 h	No K-PHI, 24 h	Red LED, 625 nm K-PHI, 24 h	K-PHI, 120 h
1	**1a**		17 (>99)	12 (>99)	2 (23)	6 (55)
2	**1b**		10 (>99)	2 (56)	7 (62)	14 (91)
3	**1c**		11 (94)	<1 (5)	3 (45)	5 (46)
4	**1d**		7 (90)	0 (70)	3 (56)	3 (96)
5	**1e**		<1 (37)	0 (0)	1 (31)	2 (65)
6	**1f**		45 (80)	<1 (16)	10 (22)	84 (84)
7	**1g**		38 (40)	0 (0)	6 (11)	25 (26)
8	**1h**		58 (>99)	>99 (>99)	4 (17)	16 (35)
9	**1j**		47 (88)	0 (0)	0 (0)	0 (5)
10	**1k**		40 (83)	0 (0)	0 (8)	14 (35)
11	**1l**		20 (47)	1 (17)	1 (20)	7 (41)

[a] Conditions: oxime (50 μmol), K-PHI (5 mg), MeCN (2 mL), O₂ (1 bar). Conversion and yield values were obtained using qNMR data.

ChemPhotoChem

Articles
doi.org/10.1002/cptc.202100088

Chemistry Europe
European Chemical
Societies Publishing

The investigation started from varying the conditions of **1i** conversion into **2i** (Figure 2). Taking into account extensive study of photochemical (without added catalyst) C=X bonds cleavage under visible light irradiation,[21,22] four sets of experiments were performed under blue (461 nm), green (525 nm) and red (625 nm) LED irradiation, as well as the control set in the dark.

From the obtained results, we may conclude that reaction is purely photochemical under blue and green irradiation. Moreover, the yields in experiments with K-PHI are greatly decreased probably due to follow up oxidation of coumarin **2i** by $^1O_2$. On the contrary, under red light we observe photocatalytic process as absence of K-PHI yields only traces of the ketone **2i**. As expected, the reaction becomes sluggish in dark or under inert atmosphere signifying role of O_2 in this reaction. Fluorescence quantum efficiency of **1i** is 0.07%, while that of **2i** is 2.2% which can be observed by naked eye (Figure S8).

To check the possibility of utilizing O-substituted oximes in the reaction, we synthesized O-benzyl (**1i-Bn**) and O-methyl

(**1i-Me**) derivatives of oxime **1i** and performed the reactions under irradiation with blue and green light (Figure 3).

Despite **1i** gave **2i** with 40% yield, O-alkyl oximes **1i-Bn** and **1i-Me** show negligibly low reactivity when the reaction was performed either in the presence of K-PHI and O_2 or without the photocatalyst under Ar. Such results point that presence of O–H proton is crucial for the cleavage of C=N bond.

To unambiguously define the reaction as a photochemical or photocatalytic process, we studied the oxidation of oximes **1a–h** under the set of conditions (Table 1).

The outcome of the reaction is not uniform, and it depends on the structure of the initial oxime. Aromatic character of a starting oxime certainly renders the process to be mostly photochemical. However, the presence of K-PHI catalyst allows the reaction to proceed more selectively towards a parent carbonyl compound under blue light irradiation in most cases except for the aromatic ketone **1h**. The nature of the oxime group (whether it is derived from an aldehyde or a ketone) also has a significant influence on the course of the reaction. Thus, ketoximes **1f–h** show good selectivity and moderate yields of the corresponding ketones **2f–h** under K-PHI catalysis under red light, while aliphatic aldoxime **1d** demonstrates poor conversion to the target aldehyde **2d** in case of K-PHI catalysis or purely photochemical process both under blue and red light irradiation. Highly positive potential of the valence band ($+2.2$ V vs NHE)[14] might be responsible for follow up oxidation of ketones or competitive side oxidation reaction of the oximes. In addition, hydrolysis of oxime is fairly easy even with trace amount of water. In case of **1g**, the observed virtually higher selectivity, when reaction was performed under red light for 120 h compared to 24 h, we explain by the precision of qNMR analysis of ca. 5% (related mainly due to the precision of peak integration).

To explore applicability of the reaction for conversion of aliphatic ketoximes, acyclic substrates **1j–l** containing branched alkyl groups were investigated. It was found that presence of bulky substituents in oxime group proximity severely decreases both conversion and yield, which narrows synthetic scope. At the same time, results indicate that direct interaction of oxime group C=N bond with oxygen may be essential for the reaction to proceed.

Absorption spectra of **1i** and its O-alkyl derivatives show no overlap between the bands of molecules and LEDs emission range (Figure 4a), which indicates that sensitization of oxime is not the key step in the process and the reaction most likely proceeds via photoactivation of oxygen.

To identify the nature of a mechanism, we conducted both static and time-resolved fluorescence quenching studies of K-PHI. Steady-state Stern-Volmer experiment was conducted with a variable concentration of **1i** (Figure 4b), and slope constant K_{SV} is calculated to be 155.353 ± 2.098 M^{-1}.

According to the reported data for O-substituted oximes with iridium bipyridyl catalysts,[23–25] the steady-state quenching is usually 1 to 3 orders of magnitude less intense for oximes bearing no additional redox-active functionalities such as unsaturated C–C bonds and aromatic rings. This data indicates
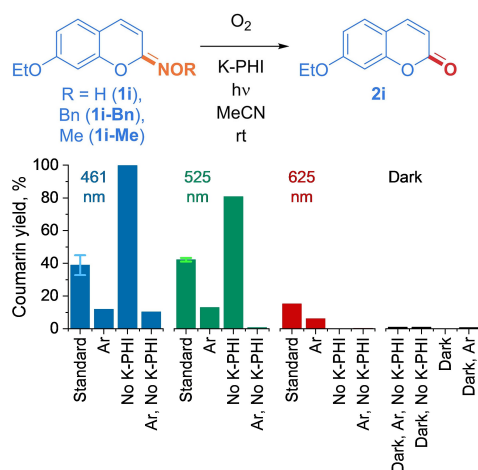
Figure 2. Set of reaction conditions for oxime **1i** conversion into ketone **2i** (standard conditions: substrate (50 µmol), K-PHI (5 mg), MeCN (2 mL), O_2 (1 bar), light irradiation, 24 h; yield values are based on quantitative NMR (qNMR) data). Error bars represent average $\pm$ std (n = 2).
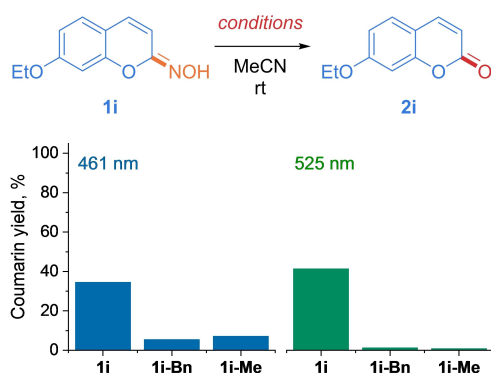
Figure 3. Comparison of O-unsubstituted (**1i**) and O-alkyl (**1i-Bn**, **1i-Me**) oximes reactivity (conditions: substrate (50 µmol), K-PHI (5 mg), MeCN (2 mL), O_2 (1 bar), light irradiation, 24 h; yield values are based on qNMR data).

ChemPhotoChem

Articles
doi.org/10.1002/cptc.202100088

Chemistry
Europe
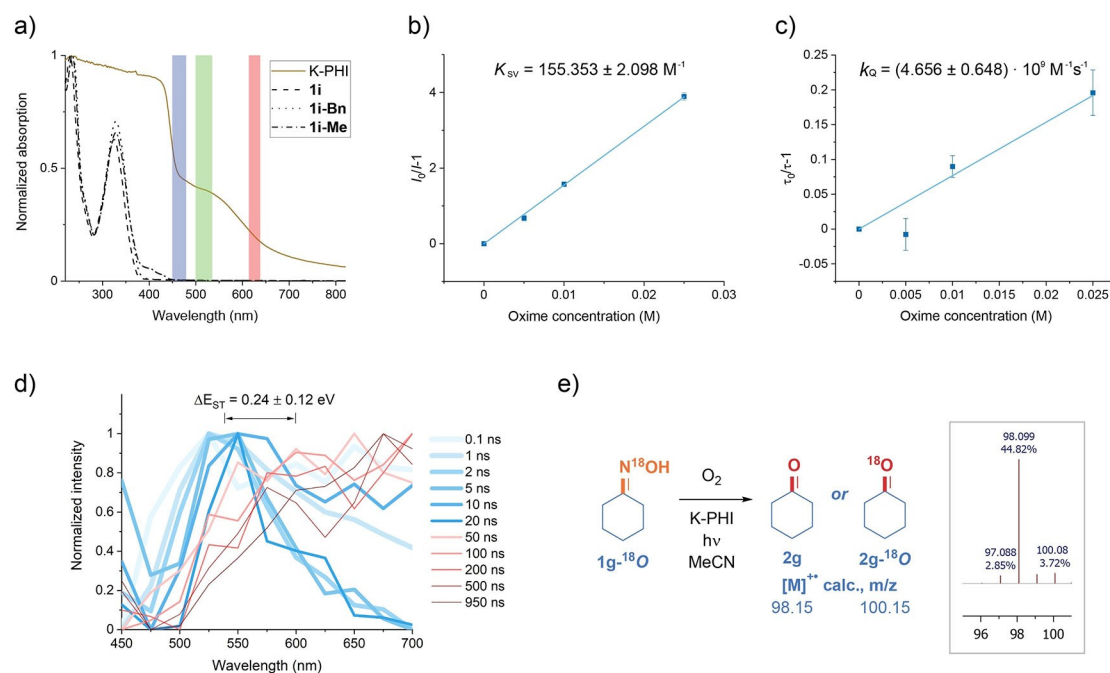European Chemical
Societies Publishing

Figure 4. Mechanism study. a) Normalized UV-Vis-NIR absorption spectra of **1i**, **1i-Bn**, **1i-Me** and K-PHI with the emission bands of the used LEDs (band width is shown approximately as the emission half-peak width). b) Stern-Volmer plot derived from steady-state emission spectra of **1i**. $\lambda_{exc} = 375$ nm. Error bars represent average ± std (n = 3). c) Stern-Volmer plot derived from time-correlated single photon counting-time resolved emission spectroscopy (TCSPC TRES) of **1i**. $\lambda_{exc} = 375$ nm. Error bars represent average ± std (n = 3). d) Determination of K-PHI singlet-triplet energy gap. e) Labelled oxygen-18 experiment and spectrum fragment of ketone product GC-MS fraction.

that sole activity of C=N bond is insufficient for the reaction to occur, which, alongside with our reactivity data (Table 1), may serve as an evidence of necessity of singlet oxygen to initiate the reaction; a conjugated π-system only facilitates possible photoredox reactions, both main and side ones alike, probably due to involvement of aromatic ring in redox processes.

We utilized **1i** as a quencher in time-resolved fluorescence measurements to determine the fluorescence quenching rate constant. Rate constant k_Q is found to be $(4.656 \pm 0.648) \cdot 10^9$ M^{-1}s^{-1} in this case (Figure 4c), which is comparable to the diffusion-limited reaction rate in diluted solvent media.[26,27] This means quenching is possible only in a rather tight contact by orbital overlapping, unambiguously defining the reaction to proceed via the Dexter mechanism. Indeed, it is reported[28,29] that for ruthenium catalysts, for instance, singlet oxygen quenching also proceeds via Dexter energy transfer.

The singlet-triplet energy gap ΔE_{ST} of K-PHI suspension was determined from emission decay curves with a delay time ranging from 0.1 to 950 ns (see SI for details, Figure S6–S7). The emission maximum progressively shifts from ca. 530 nm for short time delays, < 20 ns, which could be regarded as fluorescence (radiative relaxation of K-PHI singlet excited state) to > 600 nm for longer time delays, > 20 ns, which in turn could be ascribed to phosphorescence (radiative relaxation of K-PHI triplet excited state characterized by longer lifetime, Figure 4d). The spectral maxima were then used to calculate singlet-triplet energy gap to be 0.24 ± 0.12 eV, which is close to our previous value of 0.2 eV for solid K-PHI[16] and is in upper range for reported carbon nitrides.[30,31] Intersystem crossing

rate constant is in inverse proportionality with singlet-triplet energy gap (ΔE_{ST}), meaning lower value of the latter eventually promotes formation of singlet oxygen.[32] Typical ΔE_{ST} values for efficient small molecule oxygen sensitizers are in the range of 0.75 to 0.2 eV,[33–35] thus, K-PHI demonstrates comparable or better sensitizing efficiency in terms of energy conversion, which is supported by a low fluorescence internal quantum efficiency of 0.072%,[16] however, relatively low absorption of light with wavelengths higher than 550 nm leaves room for the catalyst improvement. The overall Jablonski diagram for K-PHI suspension is shown on Figure 5(a).

Isotope label experiment with **1g-^{18}O** (Figure 4e) demonstrates that the major product of deoximation is non-labelled cyclohexanone **2g**, evidencing the [2+2]-addition of singlet oxygen with subsequent elimination of nitrous acid. We directly observed phosphorescence of $^1O_2$ at 1271 nm in our previous work under conditions very similar to that used in the present study.[16] However, the GC-MS fraction also contains 7.7% of the labelled ketone **2g-^{18}O**, corresponding to a 12% ^{18}O isotope yield from 64%-enriched ketone, meaning a part of oxygen atoms in the product comes from the starting materials. We propose the following mechanism for this transformation (Figure 5b).

First, singlet oxygen undergoes [2+2]-cycloaddition to the oxime C=N bond. Then, assisted by O–H bond dissociation, O–O bond in the cyclic intermediate breaks. By C–N bond rotation, the cycle could be restored with ^{18}O incorporation and then undergoes consequent elimination and addition of labelled oxygen in different position to form C-^{18}O bond.
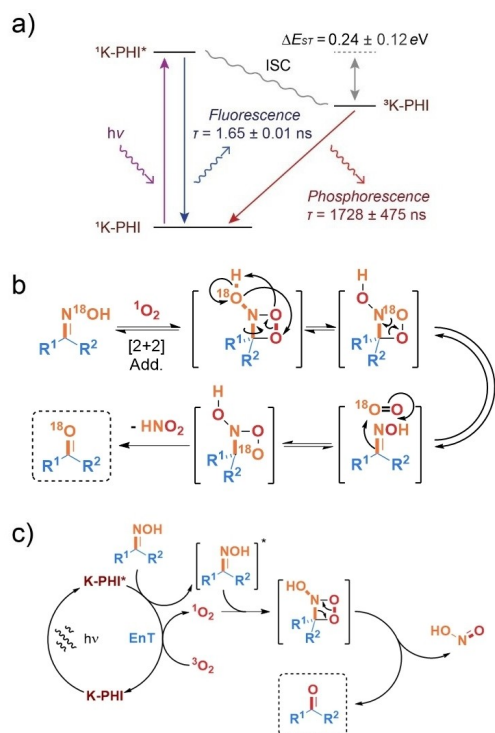
Figure 5. Energy transfer and overall reaction mechanism. a) Jablonski diagram for K-PHI in MeCN (2.5 mg mL^{-1}). b) Proposed mechanism for transformations of four-membered cyclic intermediate. c) Proposed deoximation mechanism.

Finally, elimination of HNO$_2$ occurs, yielding ^{18}O-ketone. According to isotope distribution in the final product, this process has no significant impact on overall reaction, which could be summarized as a scheme on Figure 5(c) where the key steps are [2+2]-cycloaddition of $^1O_2$ to C═N bond followed by extrusion of HNO$_2$.

3. Conclusion

Our investigation of potassium poly(heptazine imide)-catalyzed photoredox deoximation started with a set of control experiments on coumarin oxime proto-fluorescent probes. It was found that the reaction is photocatalytic under red light; under green and blue irradiation, the process is mainly photochemical. Then, the scope of reaction was expanded to include aliphatic and aromatic ketoximes in addition to electron-rich aldoximes from our previous studies. The results of qNMR experiments demonstrate that neighbouring aromatic ring induces oxime photoreactivity, but at the same time promotes undesired side reactions. Aliphatic ketoximes, on other hand, demonstrate moderate to good yields in the presence of K-PHI catalyst with enhanced selectivity under red light. Thus, this method may be suggested as a starting point procedure for chromoselective preparation of ketones from non-aromatic nitrosation products, however, the catalyst requires further improvements to effectively operate under red-shifted part of

the visible spectrum, as well as additional studies on functional group tolerance in substrates.

During our fluorescence quenching studies, we discovered that our substrate demonstrates unusually high rate of Stern-Volmer quenching which is uncharacteristic for simple oxime derivatives, and, at the same time, the rate of time-resolved quenching indicates that reaction is limited by diffusion. In this way, we got evidence for our initial guess of reaction proceeding via [2+2] addition of singlet oxygen to C═N double bond with HNO$_2$ elimination and established the Dexter mechanism for the process. To conclude our emission spectroscopy studies, we determined the singlet-triplet energy gap for K-PHI suspension in acetonitrile and compared it with reported data for carbon nitride and molecular photocatalysts for singlet oxygen generation.

Finally, to further confirm the mechanism, we carried out experiments with oxygen-18 labelled oxime. It was found out that, despite reaction mostly yielding ^{16}O-ketone, a small fraction of ^{18}O was transferred to the final product, and an explanation for this minor transformation process was proposed.

Conflict of Interest

A patent WO/2019/081036 has been filed by Max Planck Gesellschaft zur Förderung der Wissenschaften E.V. in which A.S. and M.A. are listed as co-authors.

Keywords: carbon nitride · energy transfer · oxime · poly (heptazine imide) · singlet oxygen

[1] R. C. McAtee, E. J. McClain, C. R. J. Stephenson, *Trends Chem.* **2019**, *1*, 111–125.
[2] Z. Zhang, C. Qiu, Y. Xu, Q. Han, J. Tang, K. P. Loh, C. Su, *Nat. Commun.* **2020**, *11*, 4722.
[3] D. Kong, M. Munch, Q. Qiqige, C. J. C. Cooze, B. H. Rotstein, R. J. Lundgren, *J. Am. Chem. Soc.* **2021**, *143*, 2200–2206.
[4] P. Bellotti, M. Koy, C. Gutheil, S. Heuvel, F. Glorius, *Chem. Sci.* **2021**, *12*, 1810–1817.
[5] E. R. Welin, C. Le, D. M. Arias-Rotondo, J. K. McCusker, D. W. MacMillan, *Science* **2017**, *355*, 380–385.
[6] X. Yi, X. Hu, *Chem. Sci.* **2021**, *12*, 1901–1906.
[7] N. A. Romero, D. A. Nicewicz, *Chem. Rev.* **2016**, *116*, 10075–10166.

ChemPhotoChem

Articles
doi.org/10.1002/cptc.202100088

Chemistry Europe
European Chemical
Societies Publishing

[8] W. J. Ong, L. L. Tan, Y. H. Ng, S. T. Yong, S. P. Chai, *Chem. Rev.* **2016**, *116*, 7159–7329.

[9] X. Wang, K. Maeda, A. Thomas, K. Takanabe, G. Xin, J. M. Carlsson, K. Domen, M. Antonietti, *Nat. Mater.* **2009**, *8*, 76–80.

[10] Y. Dai, C. Li, Y. Shen, T. Lim, J. Xu, Y. Li, H. Niemantsverdriet, F. Besenbacher, N. Lock, R. Su, *Nat. Commun.* **2018**, *9*, 60.

[11] J. Chen, J. Cen, X. Xu, X. Li, *Catal. Sci. Technol.* **2016**, *6*, 349–362.

[12] C. Yang, B. Wang, L. Zhang, L. Yin, X. Wang, *Angew. Chem. Int. Ed. Engl.* **2017**, *56*, 6627–6631.

[13] A. Savateev, I. Ghosh, B. Konig, M. Antonietti, *Angew. Chem. Int. Ed. Engl.* **2018**, *57*, 15936–15947.

[14] A. Savateev, B. Kurpil, A. Mishchenko, G. Zhang, M. Antonietti, *Chem. Sci.* **2018**, *9*, 3584–3591.

[15] Q. Q. Zhou, Y. Q. Zou, L. Q. Lu, W. J. Xiao, *Angew. Chem. Int. Ed. Engl.* **2019**, *58*, 1586–1604.

[16] A. Savateev, N. V. Tarakina, V. Strauss, T. Hussain, K. Ten Brummelhuis, J. M. Sanchez Vadillo, Y. Markushyna, S. Mazzanti, A. P. Tyutyunnik, R. Walczak, M. Oschatz, D. M. Guldi, A. Karton, M. Antonietti, *Angew. Chem. Int. Ed. Engl.* **2020**, *59*, 15061–15068.

[17] P. G. M. Wuts, T. W. Greene in *Greene's Protective Groups in Organic Synthesis*, Wiley VCH, **2014**, pp. 661–669.

[18] D. S. Bolotin, N. A. Bokach, M. Y. Demakova, V. Y. Kukushkin, *Chem. Rev.* **2017**, *117*, 13039–13122.

[19] Y. Tagawa, *Mini-Rev. Org. Chem.* **2011**, *8*, 186–196.

[20] S. K. Lee, M. G. Choi, S.-K. Chang, *Tetrahedron Lett.* **2014**, *55*, 7047–7050.

[21] A. J. Sanchez-Arroyo, Z. D. Pardo, F. Moreno-Jimenez, A. Herrera, N. Martin, D. Garcia-Fresnadillo, *J. Org. Chem.* **2015**, *80*, 10575–10584.

[22] A. Padwa, *Chem. Rev.* **2002**, *77*, 37–68.

[23] M. R. Becker, A. D. Richardson, C. S. Schindler, *Nat. Commun.* **2019**, *10*, 5095.

[24] Y. X. Jiang, L. Chen, C. K. Ran, L. Song, W. Zhang, L. L. Liao, D. G. Yu, *ChemSusChem* **2020**, *13*, 6312–6317.

[25] J. Chen, P. Z. Wang, B. Lu, D. Liang, X. Y. Yu, W. J. Xiao, J. R. Chen, *Org. Lett.* **2019**, *21*, 9763–9768.

[26] C. Nancoz, C. Rumble, A. Rosspeintner, E. Vauthey, *J. Chem. Phys.* **2020**, *152*, 244501.

[27] R. Chang in *Physical Chemistry for the Biosciences*, University Science Books, **2005**, pp. 347–353.

[28] B. Brunschwig, N. Sutin, *J. Am. Chem. Soc.* **1978**, *100*, 7568–7577.

[29] J. N. Demas, E. W. Harris, R. P. McBride, *J. Am. Chem. Soc.* **1977**, *99*, 3547–3551.

[30] H. Wang, S. Jiang, S. Chen, D. Li, X. Zhang, W. Shao, X. Sun, J. Xie, Z. Zhao, Q. Zhang, Y. Tian, Y. Xie, *Adv. Mater.* **2016**, *28*, 6940–6945.

[31] W. Wu, C. Han, Q. Zhang, Q. Zhang, Z. Li, D. J. Gosztola, G. P. Wiederrecht, M. Wu, *J. Catal.* **2018**, *361*, 222–229.

[32] S. Xu, Y. Yuan, X. Cai, C. J. Zhang, F. Hu, J. Liang, G. Zhang, D. Zhang, B. Liu, *Chem. Sci.* **2015**, *6*, 5824–5830.

[33] W. Shao, C. Yang, F. Li, J. Wu, N. Wang, Q. Ding, J. Gao, D. Ling, *Nano-Micro Lett.* **2020**, *12*, 147.

[34] C. Zhang, Y. Zhao, D. Li, J. Liu, H. Han, D. He, X. Tian, S. Li, J. Wu, Y. Tian, *Chem. Commun. (Camb.)* **2019**, *55*, 1450–1453.

[35] L. Wang, T. Li, P. Feng, Y. Song, *Phys. Chem. Chem. Phys.* **2017**, *19*, 21639–21647.